Modeling and Simulation of Micromachined Needles

Peiyu Zhang, G.A. Jullien
ATIPS Laboratory
University of Calgary, Calgary, AB, Canada

ABSTRACT

In this paper, the research and development of microneedles are reviewed briefly and microneedles are classified. The features of those microneedles are analyzed and discussed, and, based on analysis, a new microneedle structure is proposed. The proposed microneedle array structure uses a bi-mask process to facilitate sharp tips, a cylindric body and side ports. The proposed microneedle array has advantages over previous published results including easy fabrication and bonding, providing high needle density and robustness. In addition, the micromachined needle incorporates side ports which minimizes the potential for clogging. The microneedle array fabrication and mechanical properties are simulated with very satisfactory results.

Keywords: microneedle, out-of-plane needle, bio-mems, drug delivery, biological samples

1 INTRODUCTION

During the last two decades, it has become clear that MEMS tedhnologies offer exciting opportunities to advance the field of medicine, particularly in the area of analysis and therapy. The microbiological sample and drug delivery system are particularly well served by this technology. There are two main methods for microbiological sample and drug delivery; invasive and noninvasive methods. Each of these methods has disadvantages in their application. Recently a "minimally invasive" sampling technique using microneedles has been proposed which may eleviate some of the problems associated with microbiological sampling. The design of microneedle arrays is the subject of this paper.

Research on microneedles dates back at least to a publication by Najafi and Wise [1]. The earliest microneedles were fabricated using solid silicon, and these needles were used as microprobes for neural electrical activity recording. Following that publication, a variety of micromachined needle designs have been reported [2][3][4][5][6]. Many different approaches have been employed, including surface, bulk micromachining, LIGA, and many materials have been including silicon and metal.

The first hollow silicon microneedle was realized by Lin, Pisano and Muller [2]. In their work, a microneedle with a silicon nitride shell on top of a silicon substrate was fabricated. Henry et. al. developed a process for the fabrication of arrays of short, vertically oriented (out-of-plane) microneedles [4]. Boris Stoeber fabricated arrays of microneedles out of silicon in a similar fashion to [4] but these needles are larger and less densely packed [5]. However, a major advance was the dislocation of the centerlines of the two etches, where a bevel is produced leading to a sharp tip on one side of the needle.

The microneedle designs reported in the literature can be classified into two types: *in-plane* and *out-of-plane* microneedles. The microneedle is *in-plane* if the longitudinal axis of the microneedle is parallel to the wafer. The microneedle is *out-of-plane* if the longitudinal axis of microneedle is perpendicular to the wafer. Although the former has features of producing large needle length, the needle density is limited and the microchannel volume is very small relative to the total volume of the support silicon. The latter possesses high needle density, but most of the needles have very irregularly shaped tips, the walls of microneedle are thin and may not withstand mechanical stresses. Moreover, clogging is a problem in this type of microneedle design.

In this paper, we introduce a new microneedle design that is capable of performing microbiological sample or drug delivery. The processing method we employ uses a bi-mask technique to fabricate needles with sharp edges.

2 DESIGN AND MODELING OF THE MICRONEEDLE

In order to determine appropriate dimensions and structures of microneedles, an understanding of skin anatomy is required. Figure 1 shows the three primary layers, stratum corneum, viable epidermis and dermis. The dermis is in close contact with blood vessels and nerves. The viable epiderm is approximately 50-100 μm thick, is composed of living cells but void of blood vessels and contains few nerves. The stratum corneum, the outermost layer of skin, is 10-15 μm thick. It is primarily made of dead tissue and provides the primary barrier to penetration or transport. This signifies that a microneedle which can penetrate the stratum corneum (10-15μm) but is shorter than 50-100μm, can provide pathways for drug delivery without pain, and the needles should reach the dermis for blood samples.

The small dimensions of microneedles therefore can provide painless minimal invasion, and reduce damage to the skin. The opportunity of infection is also considerably decreased.

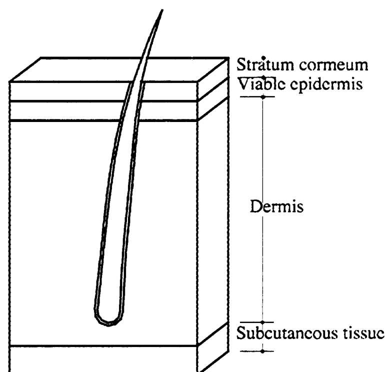

Figure 1: Skin anatomy

The needle structure mainly defines the needle's properties. Because of the small dimensions of microneedles, the fluid flow is quite small, but high needle density can compensate and increase the fluid flow rate which is a current issue with microneedles. Therefore, the needle density cannot be ignored. It is difficult for in-plane needle designs to obtain high density. In addition, we need to pay considerable attention to the fabrication material. Briefly: silicon dioxide is fragile; the strength of metal is good, but thin films of metal formed by sputtering or depositing are soft. The blockage problem must be taken into consideration when designing microneedle structures. For example, blockages are likely to occur when the inlet or outlet is on the top of the needle. In this paper we present a new Microneedle array structure that attempts to address these issues.

Fig. 2 shows the schematic drawing of the system, and Fig. 3 shows the structure of the micromachined needle array.

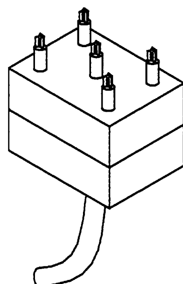

Figure 2 System Structure

The differences of our design to a recently published design [6] are as follows.

1. The side openings of the needle in [6] are produced by using an isotropic etch, this will be difficult to control because the dimension of openings is defined by the etching time. The side ports of the needle in our work are obtained by anisotropic etching. The side ports can be obtained directly by etching, which is easy to control.
2. The shape of the side pillars of the top in our work has a knife-like edge. This shape not only pierces the skin more easily than the one in [6], but also the area damaged is reduced.
3. The shape of side pillars in our design can be controlled more easily than in [6] where an isotropic etch is used. To obtain the shape of the side pillars in [6], the isotropic etching time has to be strictly controlled. There will be problems obtaining a smooth etch if there are errors in the etching time.
4. The top masks may drop during fabrication of the design in [6], which will compromise the sharpness of the tip. This problem will not occur in our design since we use a bi-mask technique.
5. If the top masks drop they may stick to the side openings, causing fabrication problems. This situation is avoided in our design.
6. Leaks may occur during application of one of the structures in [6] because the needle has no base. Although the other structure has a needle base, this base is thin in four regions where there exists a considerable stress concentration. Our structure has a needle base, and because the needle tip and needle body are produced by employing a bi-mask technique, leakage will not take place. Furthermore, the needle body in our design is cylindrical, and there is no stress concentration. Therefore, its strength is higher than the design in [6].

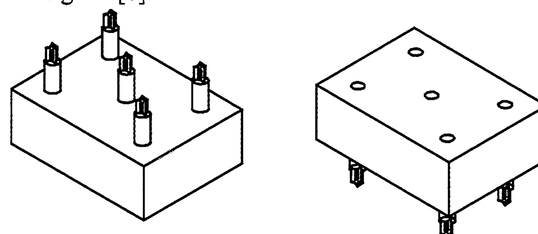

Figure 3 structure of the microneedle array

3 FABRICATION

An output from the needle construction process simulator is shown in Fig. 4.

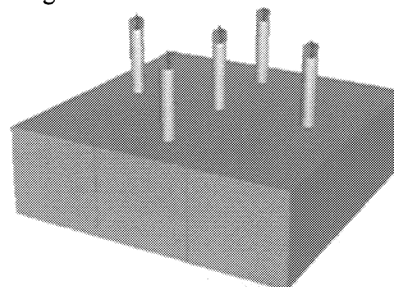

Figure 4 The Microneedle array

The fabrication process flow simulation is shown in Fig. 5. The tip and body of the needle are formed by employing a bi-mask. In the first step of the process, a silicon wafer is given a deposit of SiO_2 and patterned at the backside of the wafer (Fig. 5a). Secondly, a hole is anisotropically etched by deep RIE from the backside of the wafer, as shown in Fig. 5b. After the SiO_2 is removed, the wafer is given a thermal growth of oxide (Fig. 5c). The next step is patterning a bi-mask (Fig. 5d), and the bi-mask is aligned to the center of the hole on the front side of the wafer. An anisotropic ICP step follows (Fig. 5e). The body of the needle is formed at this step. After the upper mask from the bi-mask is removed (Fig. 5f), the wafer is isotropically etched by ICP (Fig. 5g). Following that, a second anisotropic ICP is carried out. During this step, the side ports are formed (Fig. 5h). In order to acquire the sharp needle tip, a second isotropic ICP is employed (Fig. 5i). Finally, the SiO_2 is etched(Fig. 5j), and the structure of the needle is released.

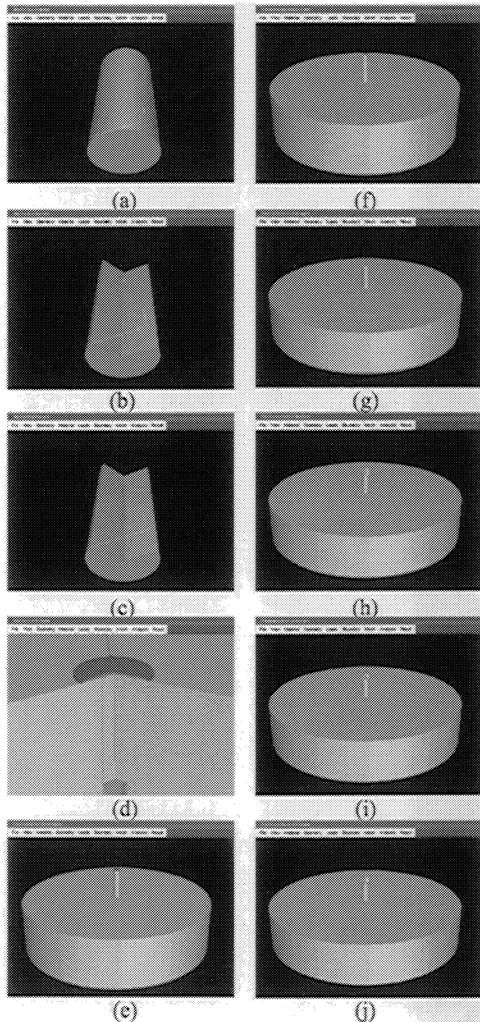

Figure 5: Process flow of the microneedle fabrication

4 SIMULATION

Since silicon is a brittle material and the needle is a long cylinder, the length of the needle is long relative to the diameter of the needle, there are two possible failure styles in terms of microneedles in our work during the insertion of the microneedles into the skin; fracture or buckling. Failure will occur when the load causes either fracture or buckling.

The fracture force can be estimated from equation (1) when the needle is loaded.

$$P_{fr} = \sigma_{fr} \quad A \qquad (1)$$

where P_{fr} is the fracture load, A is the cross sectional area of the needle, and σ_{fr} is the fracture stress of single crystal silicon[7].

The buckling load may be obtained from Euler's equation [7]. That is,

$$P_{cr} = \frac{\pi^2 EI}{CL^2} \qquad (2)$$

where P_{cr} is the critical load, L is the height of the Microneedle, C is a coefficient of the end condition. E is the modulus of elasticity for silicon, and I is the moment of inertia across the needle's cross section.

C is 4 when the needle is fixed at one end and the other end is free to move; C is 0.49 when the needle is fixed at one end and the other end is pinned; C is 0.25 when the needle is fixed at both ends.

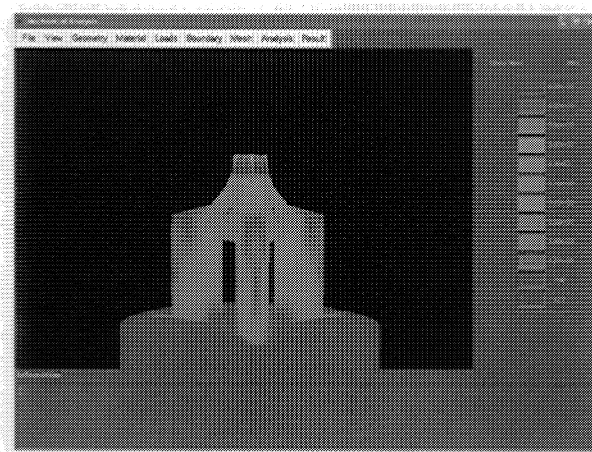

Figure 6 a) Simulation results

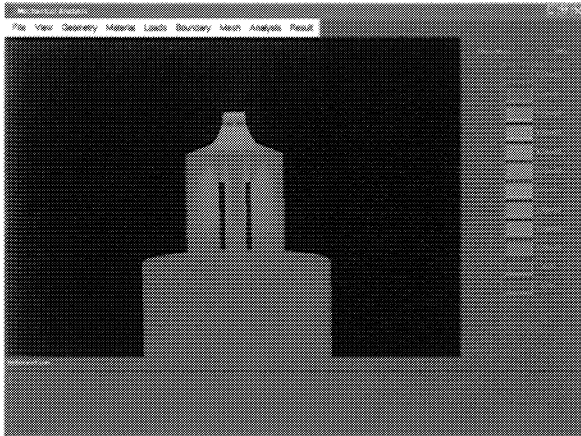

Figure 6 b) Simulation results

We have used the INTELLISUITE™ simulator to simulate the mechanical properties of our microneedle design. The simulation results of two needles of differing sizes are shown in Fig. 6 a) and b). Employing typical needle sizes in this work, our estimates of fracture force are 114μN and 400 μN respectively.

5 DISCUSSION

The needle design in this work is an out-of-plane structure, having high needle density. It is made of single silicon. The properties silicon possesses at micro scales, embodies our design with both strength and toughness. Our microneedle incorporates side ports that minimize the potential for clogging. This needle possesses high structural strength and large area of fluid exposure to the tissue. Moreover, it has a low flow resistance owing to the cylindrical channel and side ports. In addition, the needle array can be easily fabricated. The microneedle has an extremely sharp tip and the knife-like edges allow easy penetration of the skin. Because the backside of the wafer only undergoes a small amount of processing, the backside can be easily bonded with sensors, reservoirs etc.

6 CONCLUSIONS

In this paper, a novel microneedle array is proposed. Our design has several attractive features including: high needle density; low flow resistance; easy fabrication; fabrication from single crystal silicon; possesses high structural strength; provides a large area of fluid exposure to the tissue; and has an extremely sharp needle tip. Results from a simulation of the fabrication process and mechanical properties are also provided.

7. ACKNOWLEDGEMENTS

The authors acknowledge financial contributions from the Natural Sciences and Engineering Council of Canada, the Informatics Circle of Research Excellence (Alberta), and the Micronet Network of Centres of Excellence. The authors also acknowledge the equipment and software loan programs and fabrication services of the Canadian Microelectronics Corporation.

REFERENCES

[1] K. Najafi, K.Wise, T. Mochizuki. IEEE Trans. Electron. Devices, Ed-32(7), pp. 1206-1211, 1985

[2] L. Lin, A. P. Pisano and R. S. Muller, Transducers'93, Yokohama, Japan, pp. 237-240, 1993

[3] J. Chen and K. D. Wise. Solid State Sensor and Actuator Workshop, Hilton Head, S. C., pp. 256-259, 1994

[4] S. Henry, D. V. Mcallister and et al. MEMS'98, Heidelberg, Germany, pp. 494-498, 1998

[5] B. Stoeber and D. Liepmann, Proceedings of the ASME MEMS Division, 2000 IMECE, vol.1, pp. 355-359, 2000

[6] G. Patrick and S. Goran. MEMS'02, Las Vegas, NV, pp. 467-470, 2002

[7] F. P. Beer and E. R. Johnston JR, "Mechanics of materials," McGraw-Hill, 1992